Supporting Information

Novel pyrene- and anthracene-based Schiff base derivatives as Cu^{2+} and Fe^{3+} fluorescence turn-on sensors and for aggregation induced emissions

Muthaiah Shellaiah, Yen-Hsing Wu, Ashutosh Singh, Mandapati V. Ramakrishnam Raju and Hong-Cheu Lin*

*Department of Materials Science and Engineering, National Chiao Tung University, Hsinchu

30049, Taiwan (ROC)

linhc@mail.nctu.edu.tw

Table of contents:

Experimental Section

General Information

All anhydrous reactions were carried out by standard procedures under nitrogen atmosphere to avoid moisture. The solvents were dried by distillation over appropriate drying agents. Reactions were monitored by TLC plates and column chromatography was generally performed on silica gel. ^1H and ^{13}C NMR were recorded on a 300 MHz spectrometer. The chemical shifts (δ) are reported in ppm and coupling constants (J) in Hz and relative to TMS (0.00) for ^1H and ^{13}C NMR, (s, d, t, q, m, and dd means single, double, ternary, quadruple, multiple, and doublet of doublet, respectively), and d-chloroform (7.26) & (77.0), d-THF (3.58) & (66.6) was used as references for ^1H and ^{13}C NMR, respectively. Mass spectra (FAB) were obtained on the respective mass spectrometer. Elemental analysis was carried out by Elemental Vario EL. Absorption and fluorescence spectra were measured on V-670 Spectrophotometer and F-4500 Fluorescence Spectrophotometer, respectively. Identification and purity of the compounds **P1** and **A1** were characterized by NMR (^1H & ^{13}C), and Mass (FAB). Time-resolved photoluminescence (TRPL) spectra were measured using a home-built single photon counting system. Excitation was performed using a 450 and 500 nm diode laser (Picoquant PDL-200, 50 ps fwhm, 2 MHz). The signals collected at the excitonic emissions of solutions were connected to a time-correlated single photon counting card (TCSPC, Picoquant Timeharp 200). The emission decay data were analyzed with the biexponential kinetics in which two decay components were derived. The lifetime values (τ_1 and τ_2) and pre-exponential factors (A_1 and A_2) were determined and summarized. 0-14 pH buffers were freshly prepared as per the literature.[1]

Sensor titrations

Compounds **P1** and **A1** were dissolved in CH_3CN and THF at 1 x 10^{-5} M concentration. Li^+, Ag^+, K^+, Na^+, Cs^+, Ni^{2+}, Fe^{3+}, Co^{2+}, Zn^{2+}, Cd^{2+}, Pb^{2+}, Ca^{2+}, Cr^{3+}, Mg^{2+}, Cu^{2+}, Mn^{2+}, Hg^{2+}, Fe^{2+}, and Ag^{2+} metal cations were dissolved in water medium at 1x10^{-3} M concentration from their respective chloro compounds. 50% Pent methyl diethylene triamine (**PMDTA**) was dissolved in CH_3CN and THF, respectively for sensor reversibilies. For counter ion effect on Cu^{2+} and Fe^{3+} sensors responses Cu $(OAc)_2$, $Cu(NO_3)_2$, $CuCl_2$, $CuBr_2$, Cu $(ClO_4)_2$, Cu $(IO_3)_2$ and $CuSO_4$ and K_3 [Fe $(CN)_6$], $Fe(NO_3)_3$, $FeCl_3$, FeF_3, Fe $(OH)_3$, Fe $(ClO_4)_3$, Fe $(IO_3)_3$ and Fe_2 $(SO_4)_3$ were dissolved in water medium at 1x10^{-3} M concentration. However, Cu $(OH)_2$ was dissolved in NH_4OH medium at 1x10^{-3} M concentration.

General procedure[2, 3] for the synthesis of compounds P1 and A1

To 1 equiv. of aromatic amine derivatives in 50 ml of methanol, 1 equiv. of aromatic aldehyde derivatives were added with constant stirring under nitrogen and then refluxed for 12 hrs. The reaction was monitored by TLC, after completion, the reaction mixture was cooled and the solvent was evaporated to give the crude product, which was recrystallized from ethanol to afford pure compounds (**P1** and **A1**).

2-(pyren-1-ylmethyleneamino)phenol (P1): Bright yellow solid; 98% yield; ^1H NMR (300 MHz, $CDCl_3$) δ: 6.95 – 6.99 (t, J = 6.0 Hz, 1H), 7.03 (d, J = 6.0, 1H), 7.07 – 7.13 (d, J = 9.0 Hz, 1H), 7.25 – 7.50 (m, 2H), 7.96 – 8.16 (m, 7H), 8.66 – 8.71 (dd, J = 7.5 Hz, 2H), 9.60 (s, 1H (-OH)); ^{13}C NMR (300 MHz, $CDCl_3$) δ: 115.04, 115.98, 120.20, 121.63, 123.41, 125.77, 125.95, 126.03,

127.19, 128.53, 129.28, 133.41, 136.51, 152.38, 155.10; FAB: m/z = 321 (M$^+$, 100%). Anal. Calcd for C$_{23}$H$_{15}$NO: C, 85.96; H, 4.70; N, 4.36. Found: C, 85.54; H, 4.68; N, 4.35.

2-((anthracen-2-ylimino)methyl)phenol (A1): Pale-yellow solids; 71% yield; ^{1}H NMR (300 MHz, d-THF) δ: 6.95 – 7.03 (t, J = 12 Hz, 2H), 7.07 (d, J = 9.0 Hz, 1H), 7.96 – 8.27 (m, 8H), 8.71 (s, 1H), 9.13 - 9.29 (m, 2H), 12.96 (s, 1H (-OH)); ^{13}C NMR (300 MHz, CDCl$_3$) δ: 116.60, 118.35, 120.63, 123.41, 125.95, 126.03, 126.94, 127.19, 128.53, 129.28, 130.91, 131.60, 134.41, 138.91, 154.17, 156.59; FAB: m/z = 297 (M$^+$, 100%). Anal. Calcd for C$_{21}$H$_{15}$NO: C, 84.82; H, 5.08; N, 4.71. Found: C, 84.50; H, 5.07; N, 4.73.
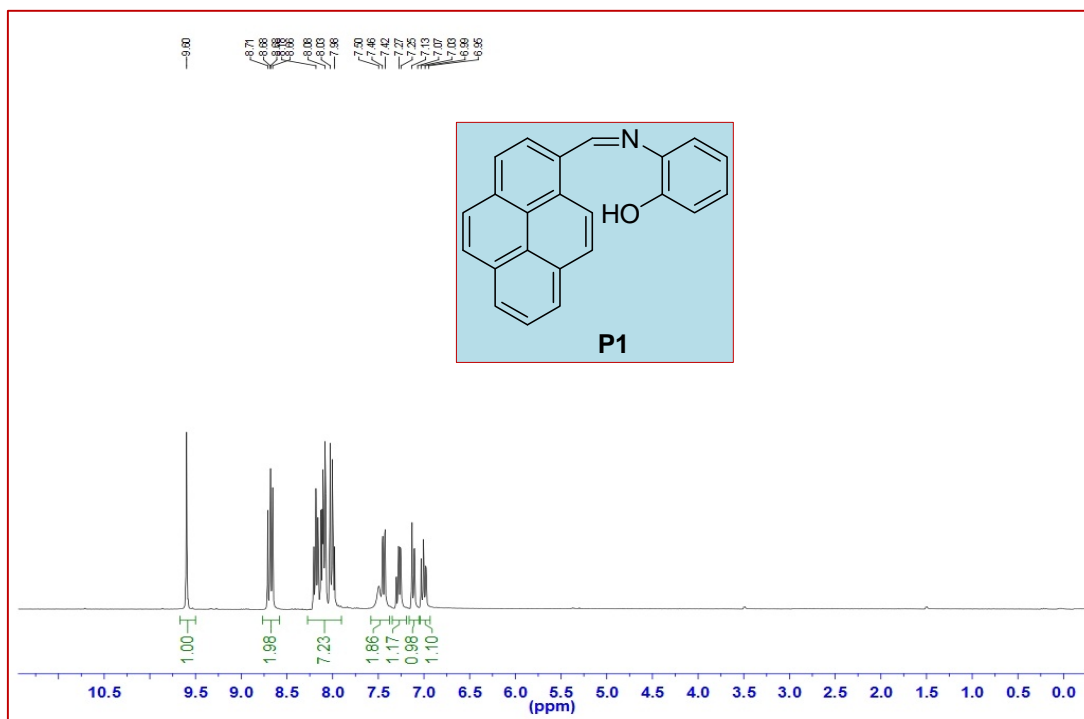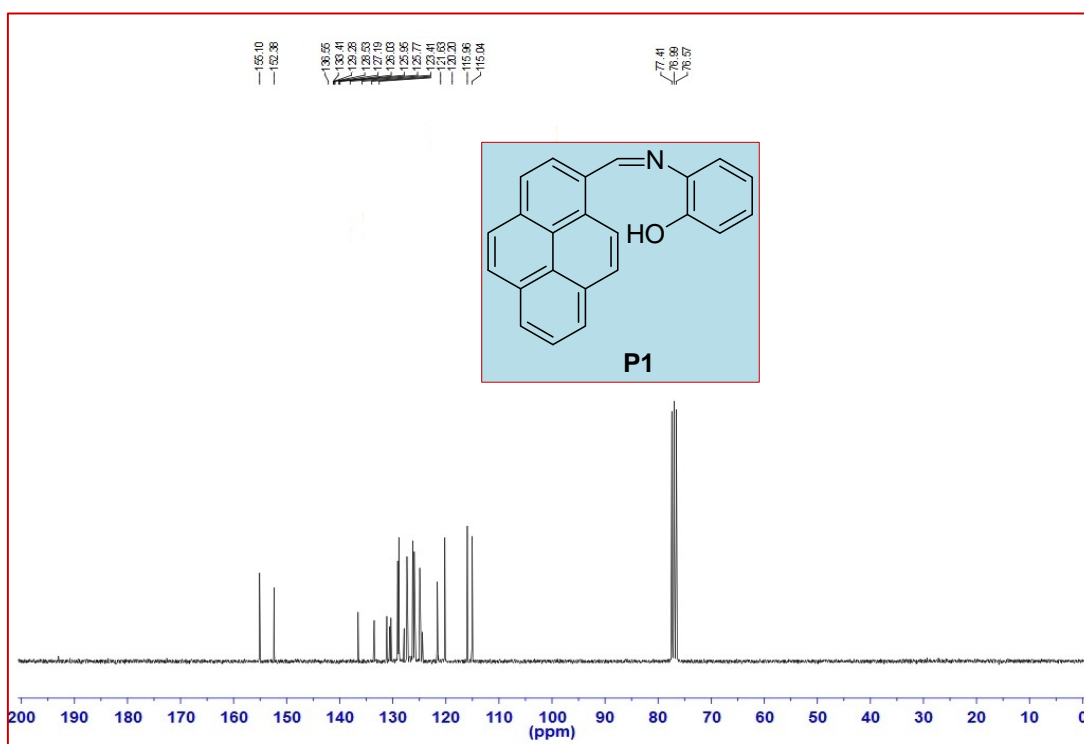
Fig. **S1** ^{1}H NMR spectrum of **P1** in d-Chloroform.

Fig. **S2** ^{13}C NMR spectrum of **P1** in d-Chloroform.
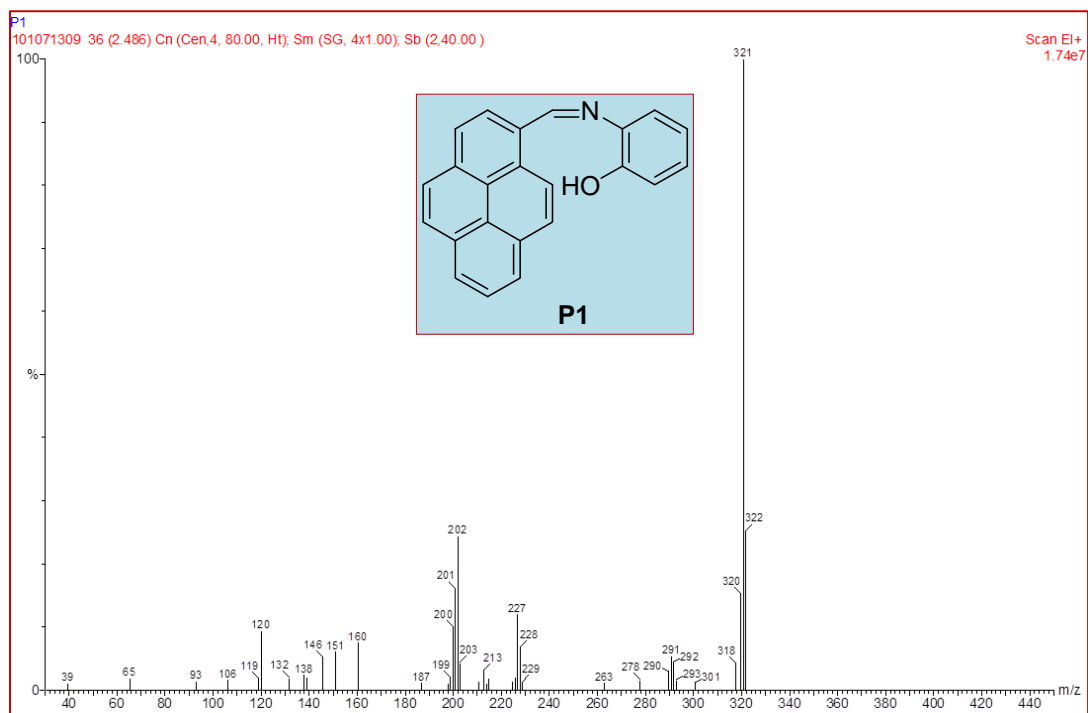
Fig. **S3** Mass (FAB) spectrum of **P1**.
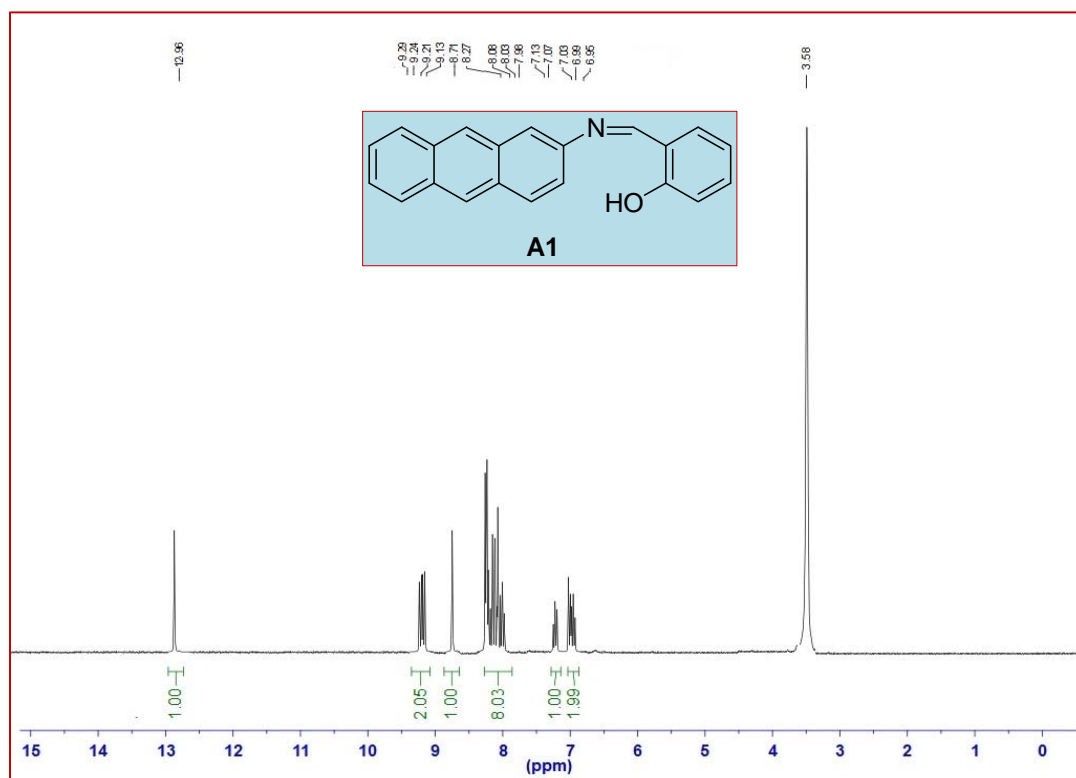
Fig. **S4** ^{1}H NMR spectrum of **A1** in d-THF.

S4
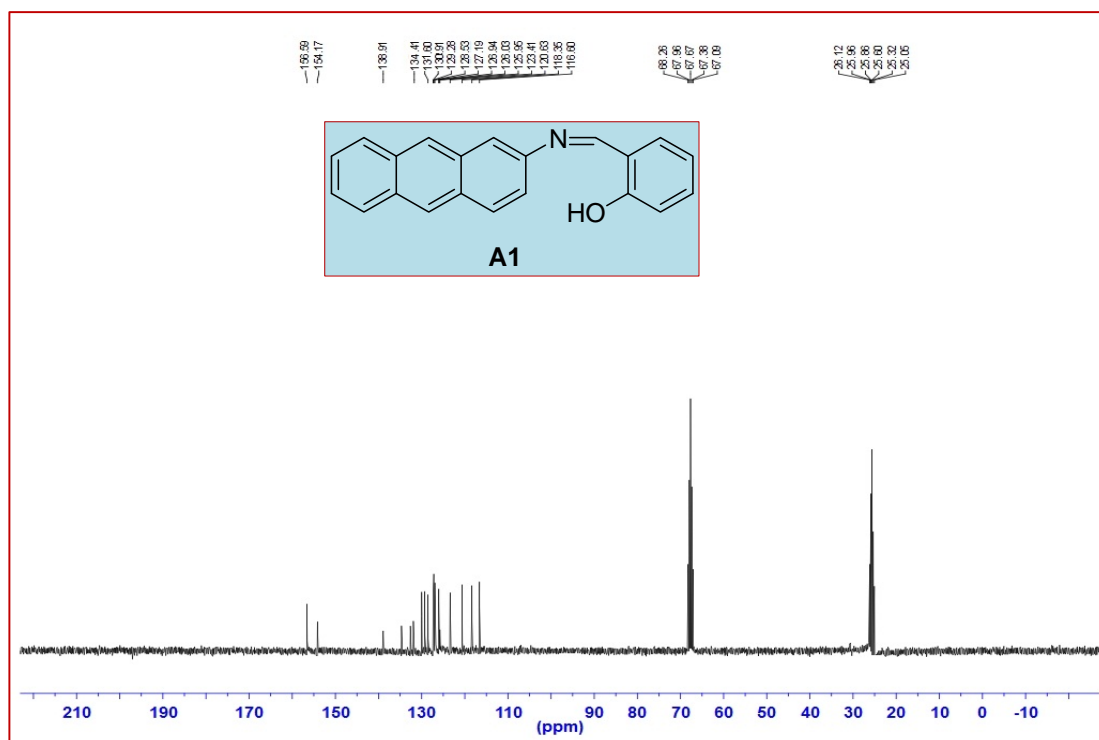
Fig. **S5** ^{13}C NMR spectrum of **A1** in d-THF.
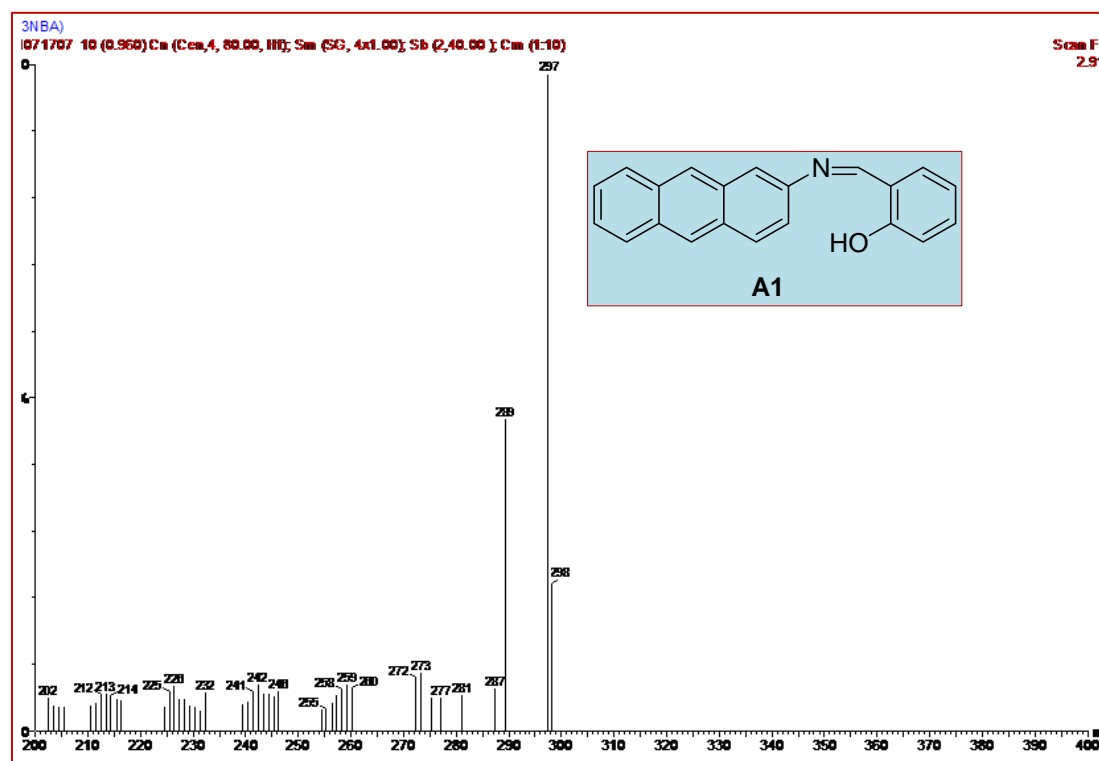
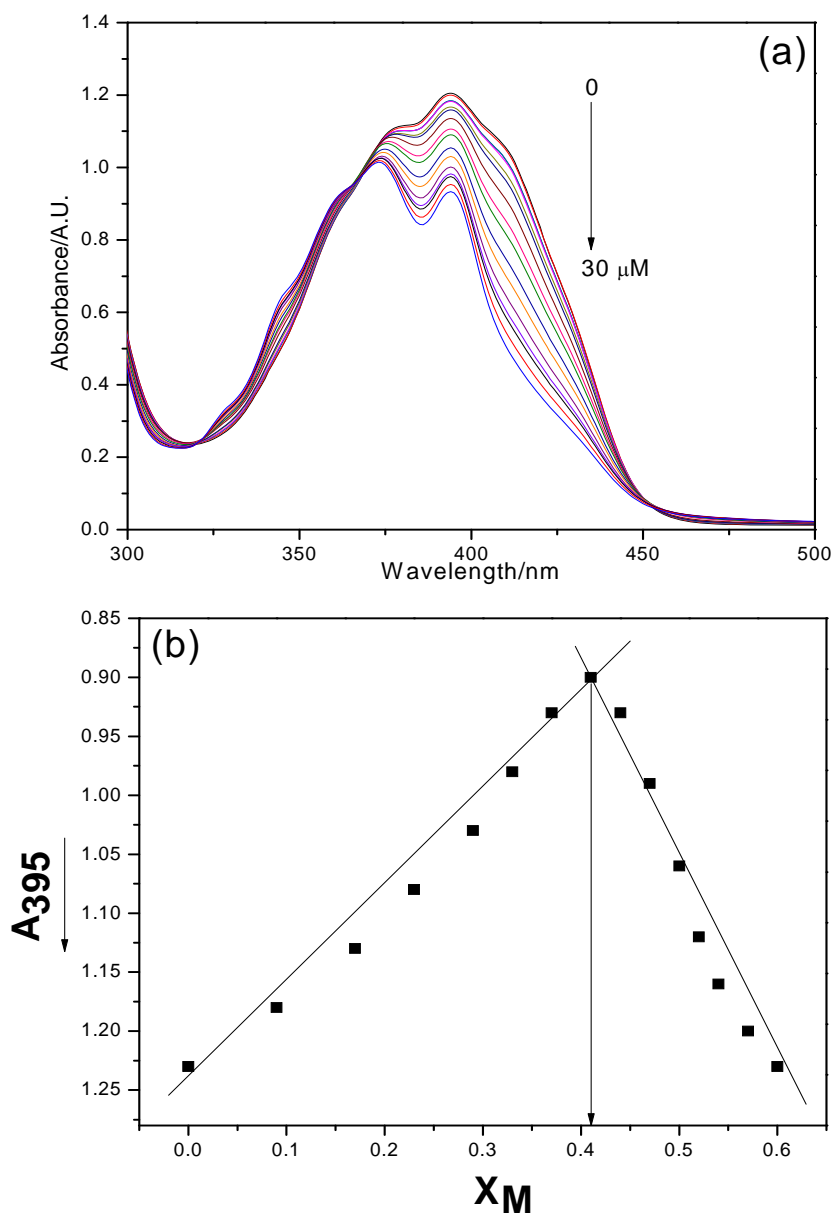**Fig**. **S6** Mass (FAB) spectrum of **A1**.

S5

Fig. **S7** Absorbance spectral changes of (a) **P1** (1×10^{-5} M) in CH_3CN, titrated with 0-30 μM (with an equal span of 3 μM) of Cu^{2+} ions in H_2O and (b) stoichiometry calculations based on absorbance changes at 395 nm; $X_M = [Cu^{2+}] / [Cu^{2+}] + [P1]$; where X_M = mole fraction, $[Cu^{2+}]$ and $[P1]$ are concentrations of Cu^{2+} and **P1**; **P1**+Cu^{2+} = 2:1 stoichiometry (ca. 0.412).
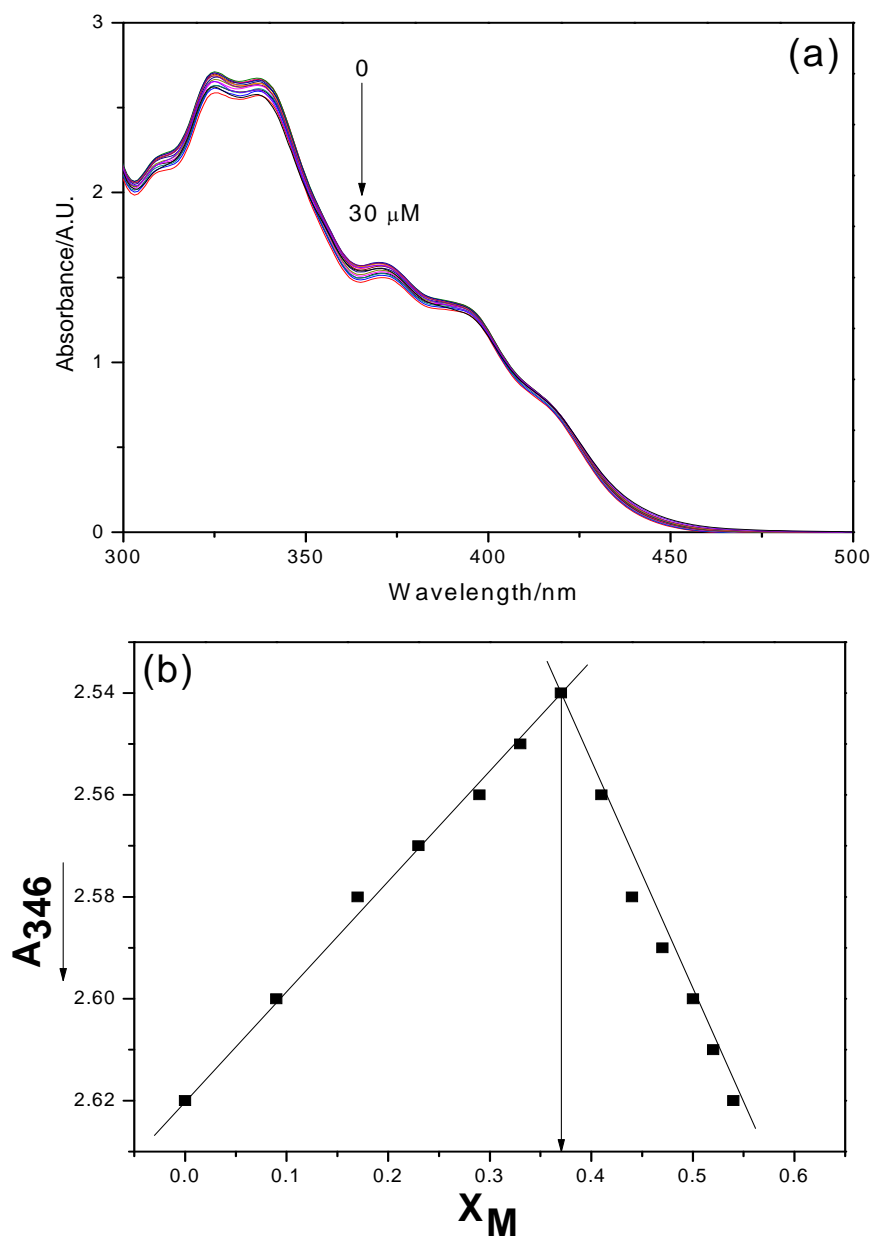
Fig. **S8** Absorbance spectral changes of (a) **A1** (1×10^{-5} M) in THF, titrated with 0-30 μM (with an equal span of 3 μM) of Cu^{2+} ions in H_2O and (b) stoichiometry calculations based on absorbance changes at 395 nm; $X_M = [Fe^{3+}] / [Fe^{3+}] + [A1]$; where X_M = mole fraction, $[Cu^{3+}]$ and $[A1]$ are concentrations of Cu^{2+} and **A1**; **A1**+Fe^{3+} = 2:1 stoichiometry (ca. 0.370).
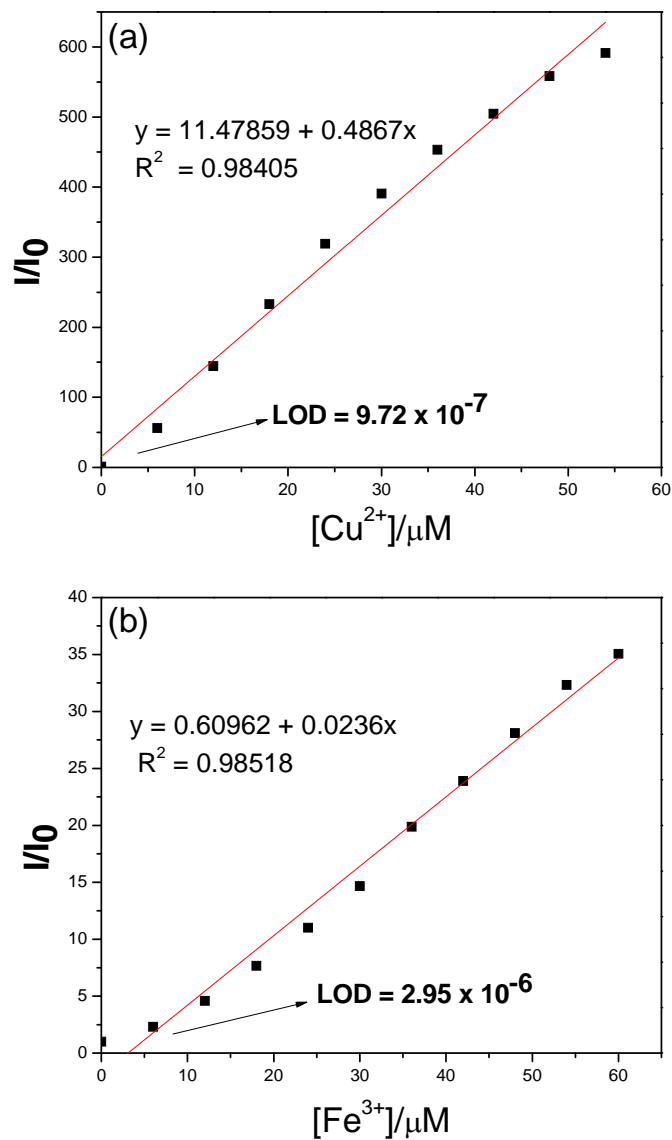
Fig. **S9** Standard deviations and linear fitting for detection limit calculations of (a) **P1** + Cu^{2+} and (b) **A1** + Fe^{2+}. [Note: Detection limit calculations were based on relative fluorescence intensity changes versus respective metal ion concentrations].
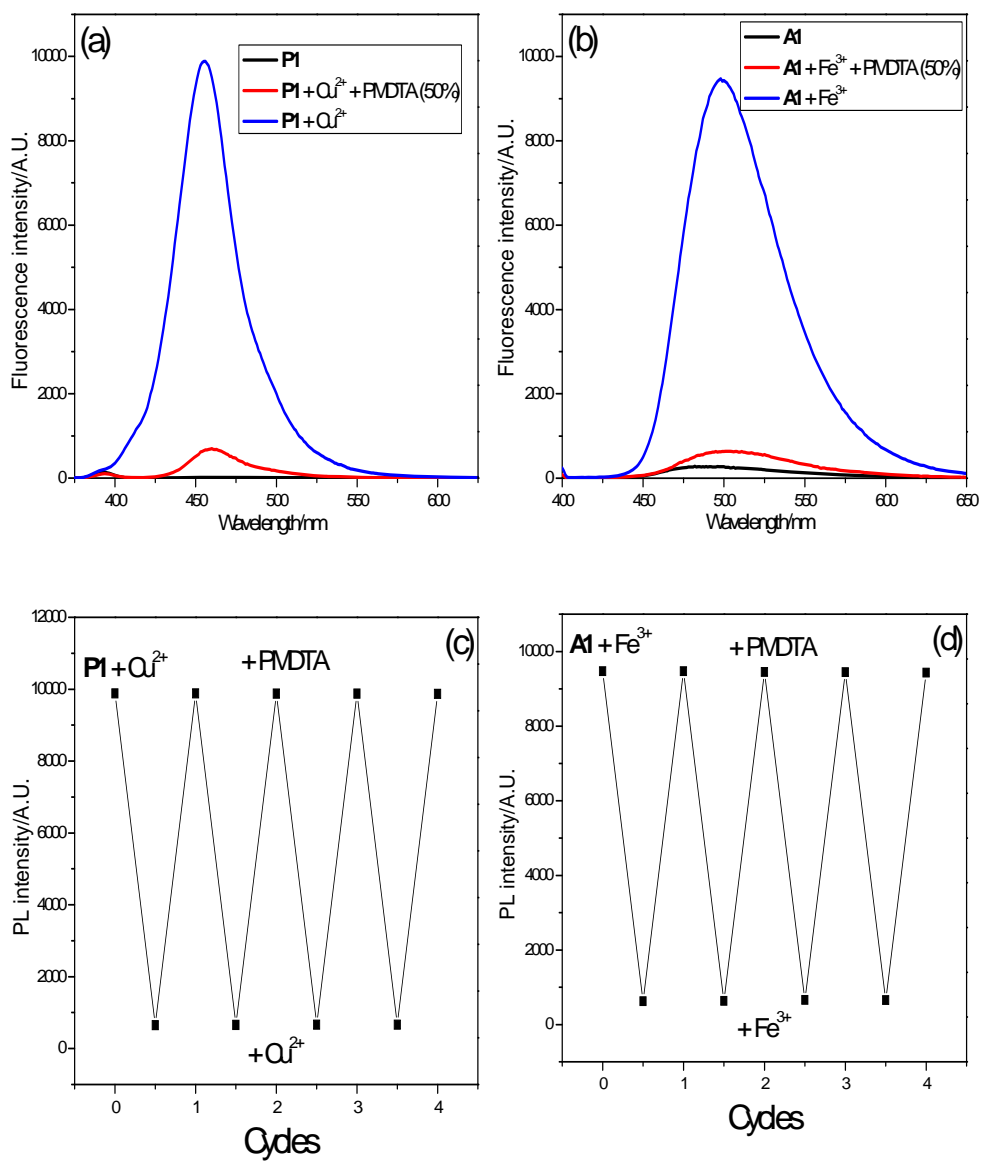
S8

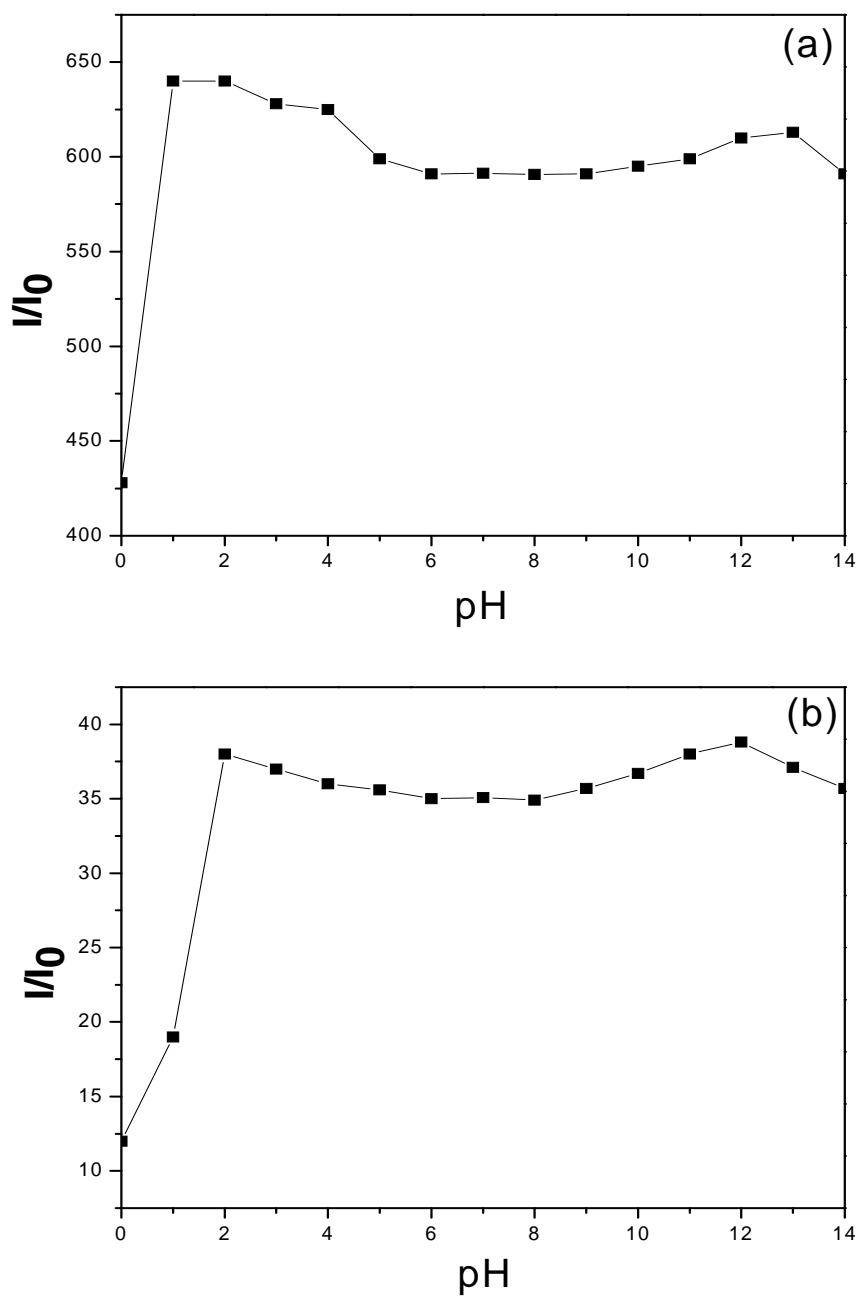**Fig**. **S10** Sensor reversibilities and reversible cycles of (a, c) **P1** + Cu^{2+} and (b, d) **A1** + Fe^{3+}.

Fig. **S11** Sensor responses of (a) **P1** + Cu^{2+} and (b) **A1** + Fe^{3+}, as a function of pHs (0-14).
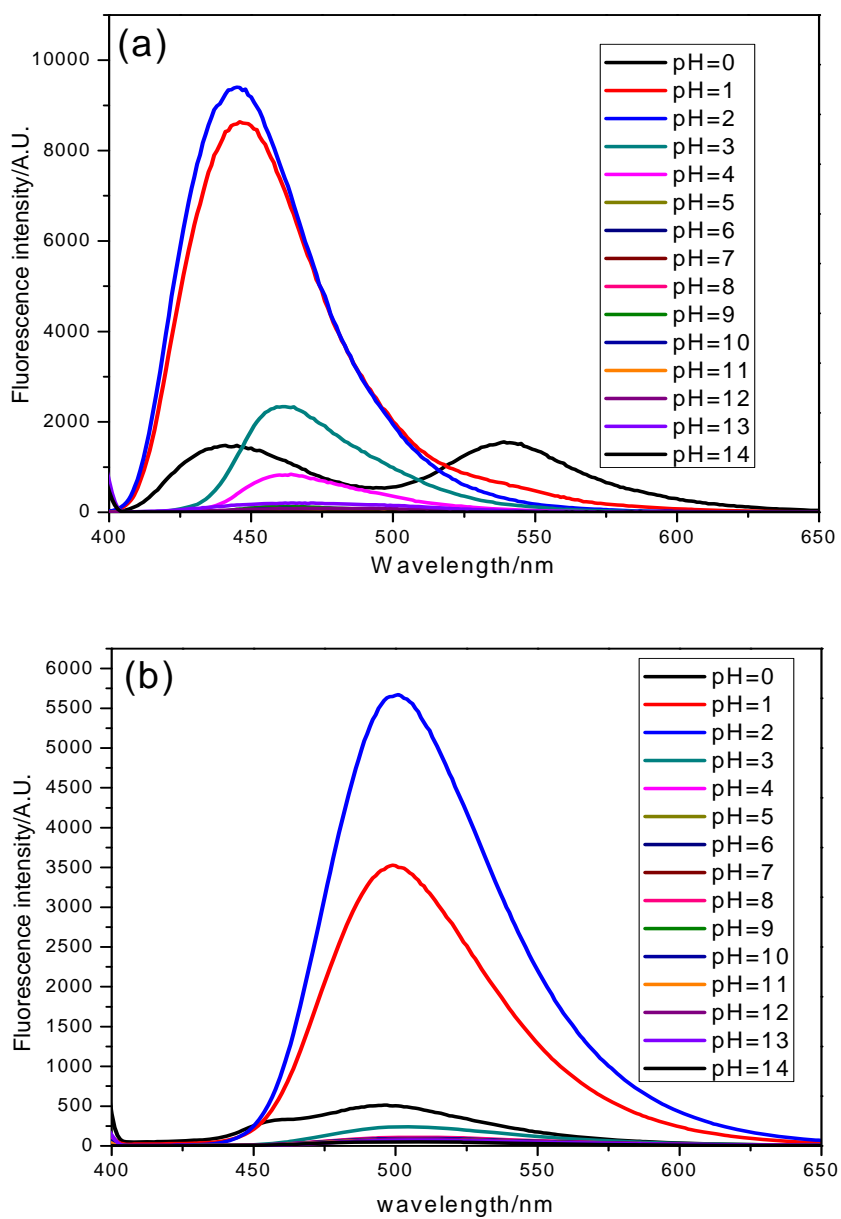
Fig. **S12** PL spectral changes of (a) **P1** (20 μM) in CH_3CN and (b) **A1** (20 μM) in THF upon the addition of 100 μM of pH (0-14) buffers in H_2O.

Determination of Association Constant:[4, 5]
Assuming a 2:1 complex formation, the association constant was calculated on the basis of the titration curves of the sensor **P1** and **A1** with Cu^{2+} and Fe^{3+}. Association constants were determined by a linear least square fitting of data with the following equation as a referenced method.

$$[Cu^{2+}] = 1/2K_a[L]_T \cdot x/(1-x^2) + [L]_T/2 \cdot x \text{ and}$$
$$[Fe^{3+}] = 1/3K_a[L]_T \cdot x/(1-x^3) + [L]_T/3 \cdot x$$

Where K_a is complex association constant; $[Cu^{2+}]$ and $[Fe^{3+}]$ are the concentrations of Cu^{2+} and Fe^{2+} ions; $[L]_T$ is the initial concentration of sample; $x=I-I_0/I_{max}-I_0$; I, I_0 and I is the absorption intensity at 455 nm (**P1**) or 495 nm (**A1**) of respective species, free ligand and the absorption intensity at 455 nm (**P1**) or 495 nm (**A1**) upon the addition of Cu^{2+} and Fe^{3+}, respectively.
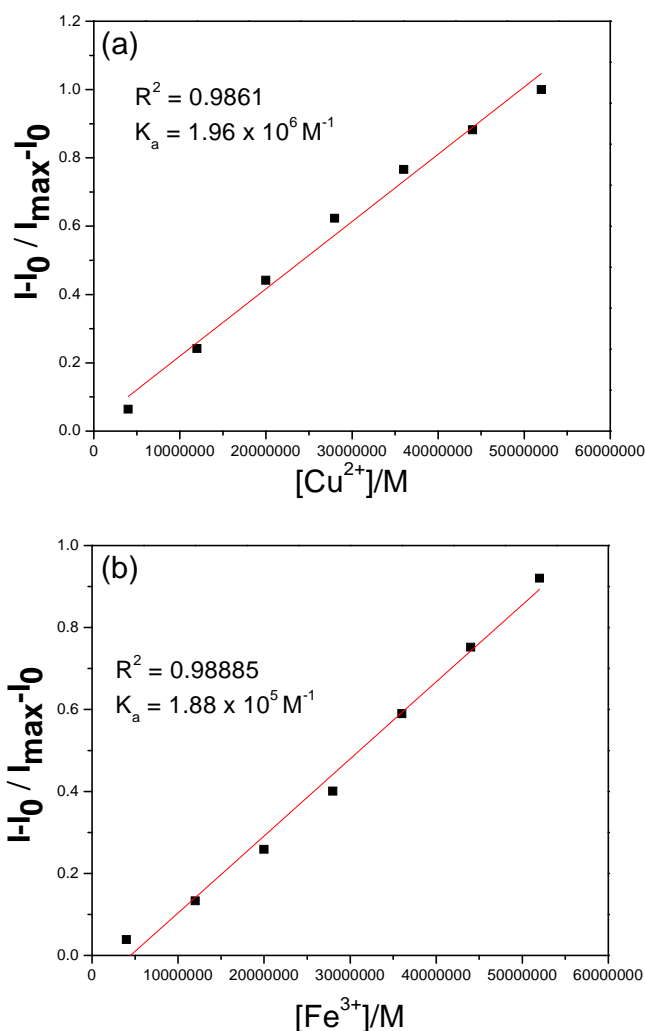

Fig. **S13** Determination of association constants of (a) **P1**+Cu^{2+} and (b) **A1**+Fe^{3+} based on linear least square fitting.
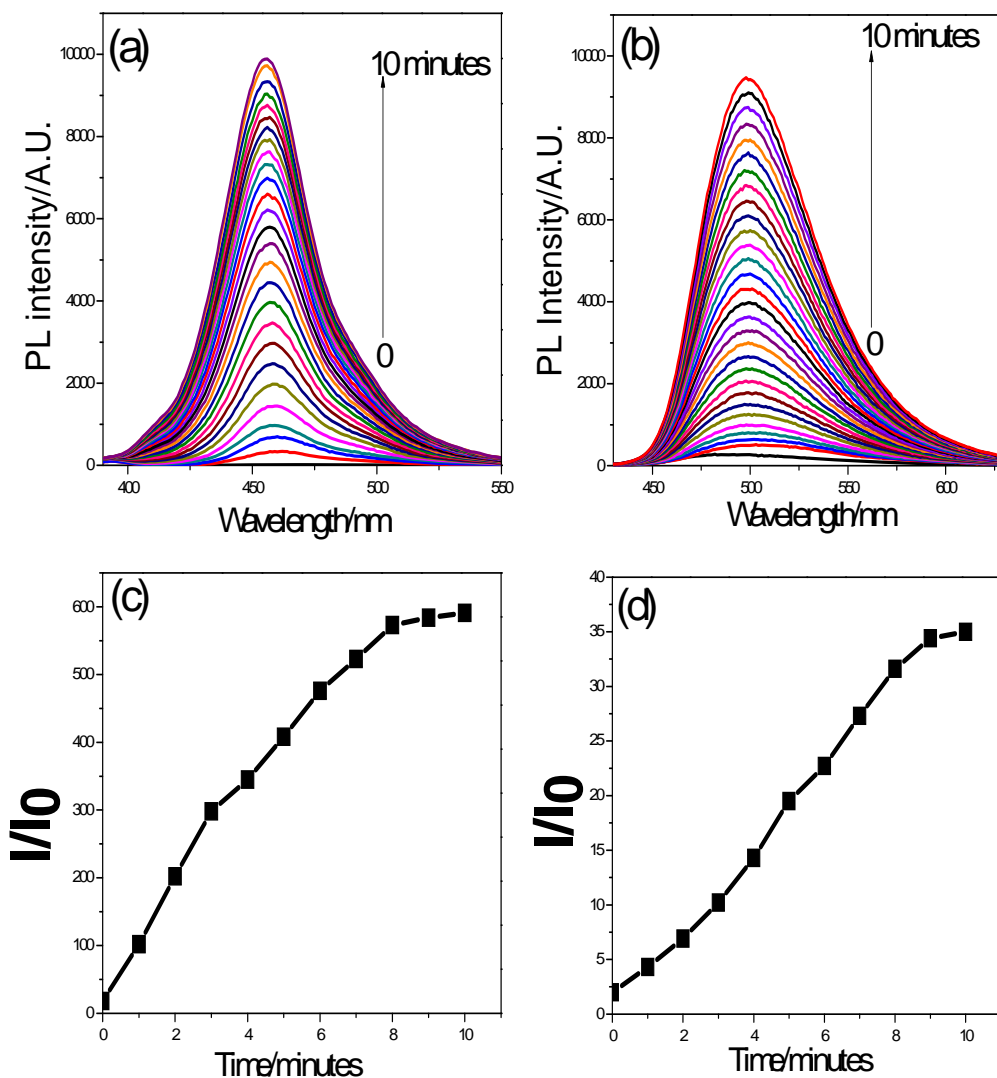
Fig. **S14** Time dependent fluorescence spectral changes of (a) **P1** (20 µM) in CH_3CN (λ_{ex} = 395 nm) with 10 µM Cu^{2+} in H_2O and (b) **A1** (20 µM) in THF (λ_{ex} = 395 nm) with 10 µM Fe^{3+} in H_2O (each measurement carried out at equal span of 20 seconds). (c and d) relative fluorescence intensity changes of **P1** and **A1**, respectively, as a function of time (0-10 min.).
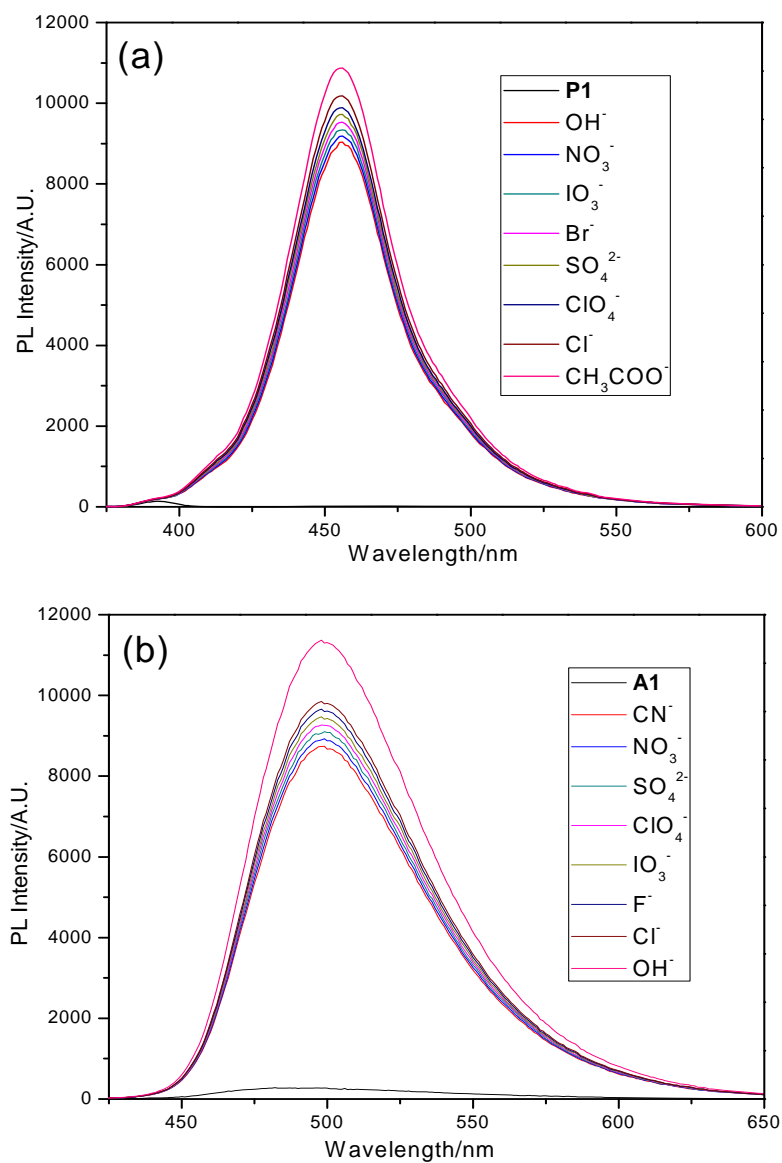
Fig. **S15** Sensor responses of (a) **P1** and (b) **A1** towards Cu^{2+} and Fe^{3+} in presence of different counter ions (for Cu^{2+} sensors CH_3COO^-, NO_3^-, Cl^-, Br^-, OH^-, ClO_4^-, IO_3^- and SO_4^{2-} and for Fe^{3+} sensors CN^-, NO_3^-, Cl^-, F^-, OH^-, ClO_4^-, IO_3^- and SO_4^{2-} were taken as counter ions)
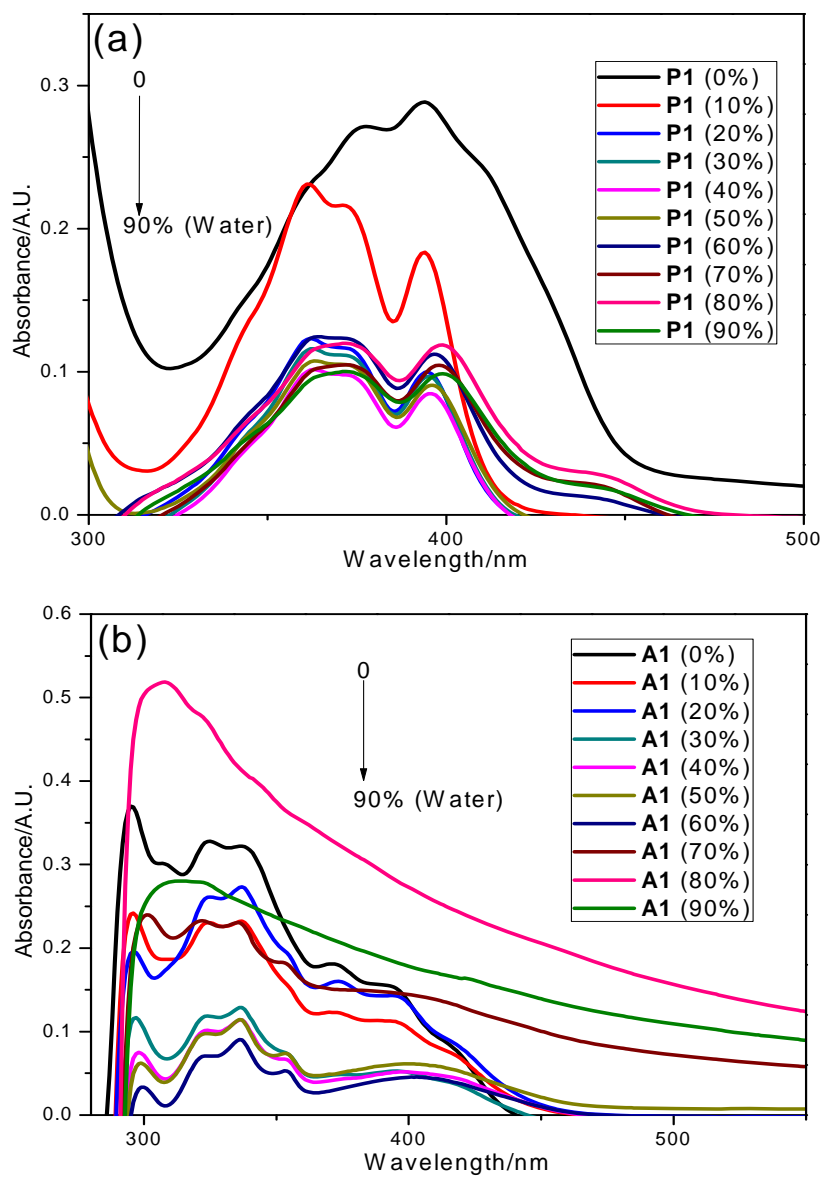
Fig. **S16** Absorbance spectral changes of (a) **P1** and (b) **A1**, upon increasing the concentration of water (0-90%) (Note: the spectra were taken after 18 hours).
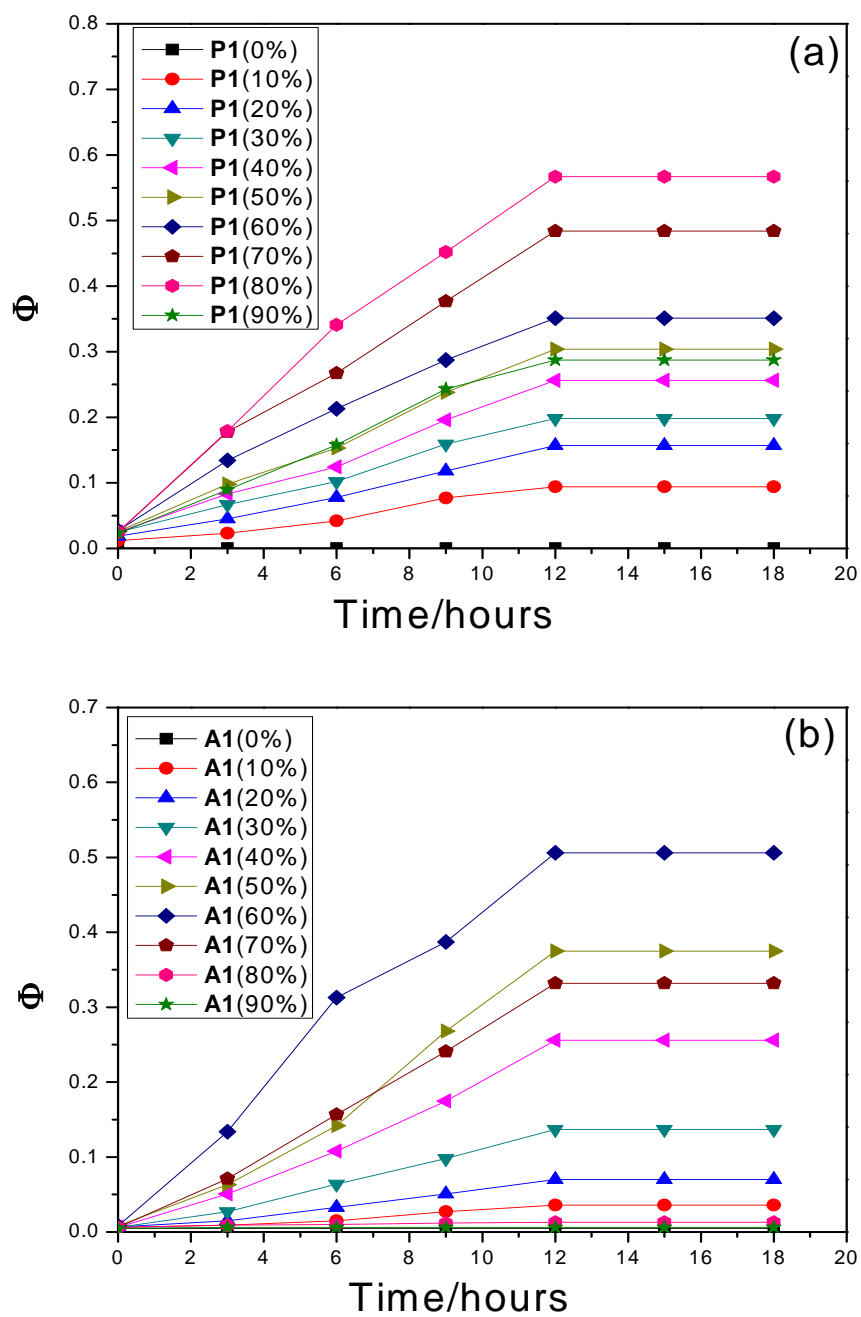
Fig. **S17** Quantum yield (Φ) changes of (a) **P1** and (b) **A1**, upon increasing the concentration of water (0-90%) as a function of time (0-18 hours).
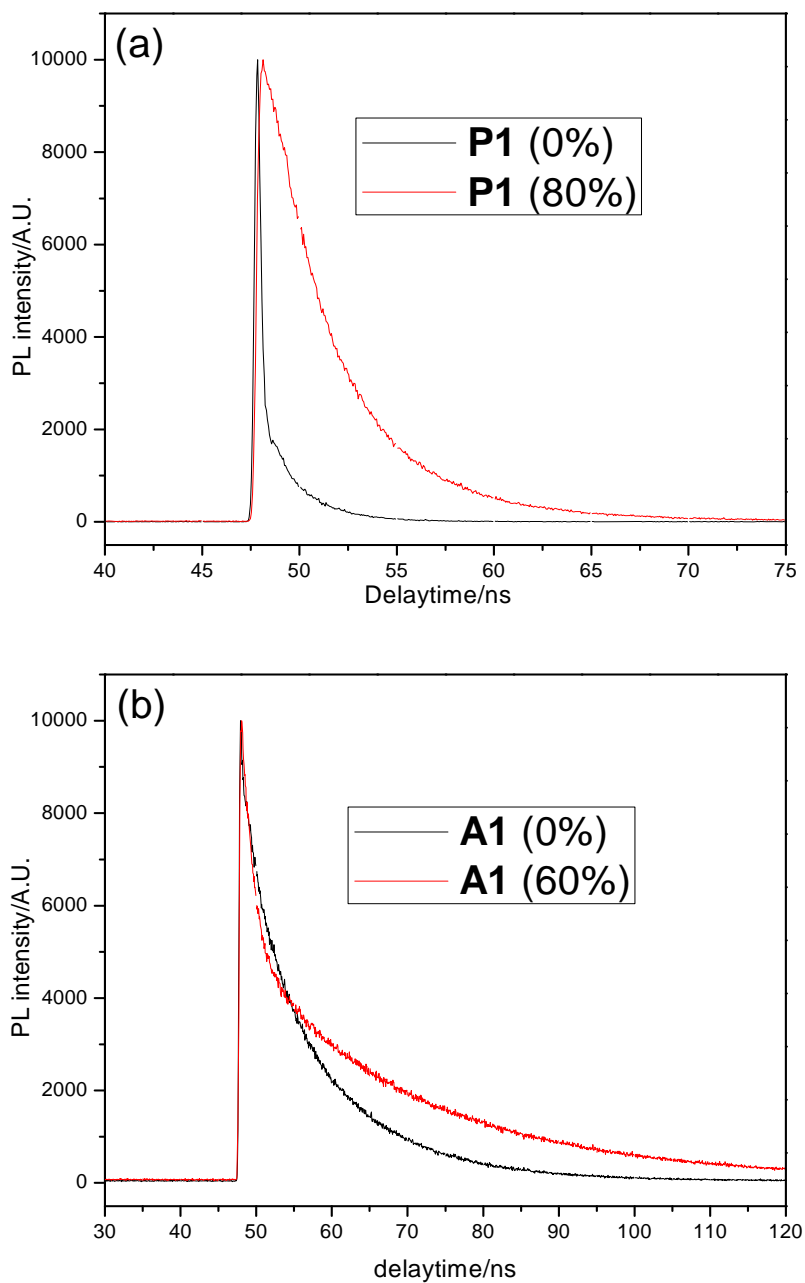
Fig. **S18** Time resolved fluorescence spectra (TRPL) of (a) **P1** in CH_3CN (0% and 80% of water) and (b) **A1** in THF (0% and 60% of water) measured after 18 hours.

Table S1. Time-resolved fluorescence decay constants of **P1** and **A1**, sensor complexes and their aggregation induced emissions concentrations.

Compound	τ_1(ns)	τ_2(ns)	A_1(%)	A_2(%)	τ_{Avg}(ns)
P1	0.2321	1.8891	35.58	64.42	1.30
P1+Cu^{2+}	1.8491	6.9600	96.16	3.84	2.05
P1 (80%)	3.2516	6.2960	71.31	28.69	4.13
A1	3.4440	11.7947	14.31	85.69	10.60
A1+Fe^{3+}	5.9450	14.0700	23.51	76.49	12.46
A1 (60%)	1.9563	24.17	8.40	91.60	22.30

Notes and References

1 R. A. Robinson, and R. H. Stokes, *Electrolyte solutions" 2nd ed., rev.*, 1968, London, Butterworths.

2 K. Krzysztof, I. and Kuzniarska-Biernacka, *Struct. Chem*., 2010, **21**, 357.

3 C. G. Freiherr von Richthofen, A. Stammler, H. Bogge, and T. Glaser, *J. Org. Chem*., 2012, **77**, 1435.

4 Q. Mei, L. Wang, B. Tian, F. Yan, B. Zhang, W. Huang, and B. Tong, *New J. Chem*., 2012, **36**, 1879.

5 Y. Kubo, M. Kato, Y. Misawa, and S. Tokita, *Tetrahedron Lett*., 2004, **45**, 3769.